Surge and High Frequency Propagation in Industrial Power Lines

François D. Martzloff
and Harold A. Gauper
General Electric Company
Schenectady NY
f.martzloff@ieee.org

Reprinted, with permission, from *IEEE Transactions on Industry Applications* IA-22, July/August 1986
First presented at IEEE ICPS, May 1985

Significance:
Part 4 – Propagation and coupling of surges

The propagation and attenuation of surges or high-frequency disturbances in power lines has been described in different terms by workers hailing from time-domain or frequency-domain schools of thought. Nature, of course, recognizes neither one in particular, and the phenomena are the same. This paper is an attempt at unification of the description, reporting measurements made on the same specimen by the two different techniques.

Unidirectional pulses with duration ranging from 200 ns to 50 μs, and the 0.5-μs – 100-kHz ring wave were injected in a metal-enclosed line as well as a non-metallic jacketed line. Data are presented in graphical form for the continuous-frequency measurements and as typical oscillograms for the pulse measurements.

From the time-domain surge measurements, it becomes apparent that long lines will attenuate single-shot impulses for very short duration (less than 1 μs), but no appreciable attenuation can be expected for longer pulses. An open-end line will produce the classical doubling effect when the line length is sufficient to contain the surge front. If the line if shorter than this value, reflections occur while the surge front is still rising, so that the doubling effect produces steps on the front but no doubling of the ultimate peak of this surge.

Surge and High-Frequency Propagation in Industrial Power Lines

FRANÇOIS D. MARTZLOFF, FELLOW, IEEE, AND HAROLD A. GAUPER, JR., SENIOR MEMBER, IEEE

Abstract—**Laboratory measurements were made on a three-conductor line, with or without steel conduit sheath (typical of single-phase 120/240-V systems), to determine the attenuation of surges and the response to steady excitation at frequencies in the range of 100 Hz–10 MHz. Line length ranged from 75 to 225 m. Impedance matching was maintained at the sending end, while at the receiving end various loads (matched or mismatched) were included. A nonlinear load was also used, illustrating the side effects of connecting a surge protective device at the end of the line.**

INTRODUCTION

THE PROPAGATION and attenuation of surges or high-frequency disturbances in power lines has been described in different terms by workers hailing from time-domain or frequency-domain schools of thought. Nature, of course, recognizes neither one in particular, and the phenomena are the same. This paper is an attempt at unification of the description, reporting measurements made on the same specimen by the two different techniques. In a second phase of this work, numerical methods would be applied to correlate and convert the data from one domain to the other.

A typical industrial power line was deployed in the laboratory, consisting of three conductors in a steel conduit. The line was folded into a zig-zag arrangement to allow both ends and two intermediate points to be within short reach of the instruments. The parameters of a three-conductor nonmetallic jacket line were also examined. Pulses of different shapes and continuous swept-frequency signals were applied at one end of the line. Measurements of voltages or currents were made to characterize the propagation and attenuation (or enhancement) of the signals.

From the measurement results, data are presented in graphical form for the continuous-frequency measurements and as typical oscillograms for the pulse measurements. Implications are discussed for application to typical situations.

LINE AND INSTRUMENTATION

The line consisted of 225 m of 20-mm (3/4-in) steel conduit, arranged in a zig-zag configuration to bring the start, the end, and two intermediate points at 75 m and 150 m close to each other, allowing connection of recording instruments without change of probe length. Three wires of 3.3 mm^2 cross section (12 AWG) were pulled through the conduit, representing the line, neutral, and grounding conductors of a typical single-phase installation. In all measurements, the neutral and grounding conductors were bonded to the conduit at the sending end, representing a typical service entrance configuration. At the intermediate points and at the far (receiving) end, the neutral was not connected to the grounding conductor. At the receiving end, the grounding conductor was also bonded to the conduit. Limited measurements were also performed on a 75-m-long line of nonmetallic three-wire conductor to investigate the differences between the "open line" configuration and the "quasi-coaxial" configuration of the conduit-enclosed line.

Because the conduit-enclosed line is practically insensitive to its surroundings, it could be zig-zagged in a steel-walled room without undue effects. In contrast, the nonmetallic jacket line might be sensitive to the proximity of walls and, very likely, to its own adjacent turns if not stretched out in "free space." To evaluate the importance of this concern, measurements were made on the three-conductor wire left in its original coiled package (50-cm average diameter) before the line was stretched out in a long hairpin shape, with only the sending and receiving ends inside the building, the rest of the line being held at least 4 m away from the building and ground. In these measurements the grounding conductor and neutral conductor were bonded at the sending end.

Surges and signals were generally injected and measured between the line conductor and the neutral conductor, across which the sensitive loads are expected to be connected. In the experiment concerned with connection effects at the line end, measurements were also made between the neutral and the grounding conductors at the end of the 75-m line, where various configurations of surge suppressors were installed.

Surges were generated by a Velonex 350 or KeyTek 711 generator, monitored by a Tektronix 7633 oscilloscope with two P6015 probes in differential mode, allowing measurements at the four access points of the line. For the fast repetitive pulses generated by the Velonex 350 generator, a trigger signal allowed synchronized sweep of the oscilloscope for all four measurements, so that propagation time would be displayed on the recordings. For single pulses generated with the KeyTek 711 generator, internal triggering of the oscilloscope in single-sweep storage mode provided the recording of the pulses. Continuous frequency measurements were per-

Paper IPCSD 85-34, approved by the Power Systems Engineering Committee of the IEEE Industry Applications Society for presentation at the 1985 Industrial and Commercial Power Systems Technical Conference, May 13–16. Manuscript released for publication March 7, 1986.

F. D. Martzloff was with the General Electric Company, Schenectady, NY. He is now with the Electrosystems Division, National Bureau of Standards, Building B 162, Room 220, Gaithersburg, MD 20899.

H. A. Gauper, Jr., was with the General Electric Company, Schenectady, NY. He is now at 826 Sanders Avenue, Scotia, NY 12302.

IEEE Log Number 8608868.

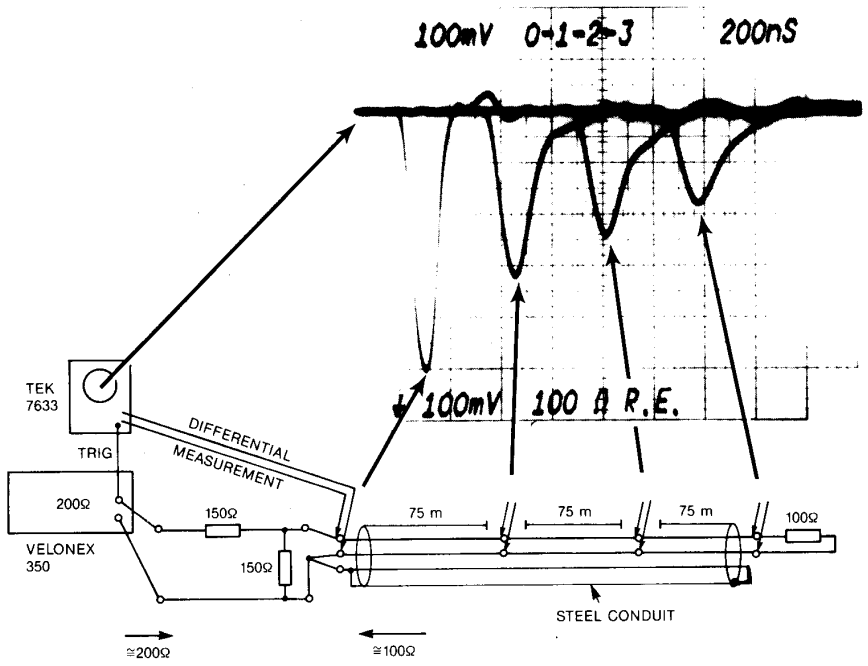

Fig. 1. Recordings at sending and intermediate points and receiving end of line, terminated with matching impedance, for 200-ns-wide pulse.

formed with a Hewlett-Packard system consisting of a Model 8553A spectrum analyzer and a 8443A tracking generator.

Surge Propagation Measurements

Four types of surges were injected into the line, with different waveforms:

- a 200-ns-wide unidirectional pulse,
- a 2-μs-wide unidirectional pulse,
- a 1.2/50-μs surge, as described by [3],
- a 0.5-μs 100-kHz ring wave, as described by [3].

A. 200-ns Pulse

Fig. 1 shows schematically the test line and a composite oscillogram of the voltages at the sending end, intermediate points, and receiving end. Note the impedance-matching network between the generator and the line, providing an optimum waveform for the generator output (200 Ω) and minimizing reflection of the surges returning from the line (100 Ω). A 100-Ω matching termination was connected at the receiving end for this recording.

The attenuation of this pulse along the line is quite apparent, with an average 0.7 ratio between the voltages of points separated by 75 m of line. The propagation time for the 225 m can be seen as 1.1 μs.

Fig. 2 shows the propagation of the same 200-ns-wide pulse with open-ended line. The voltage enhancement at the receiving end (3.75 divisions compared to the 1.9 divisions in Fig. 1) illustrates the classical doubling effect at the open end. In spite of this doubling effect, enough attenuation of the short spike occurs over the total 225 m of the line that the pulse at the receiving end is lower than that at the sending end. For a line length of 150 m, the doubling effect would result in a receiving-end crest of $2 \times 2.5 = 5$ divisions, i.e., equal to the sending-end pulse. For a line length of 75 m, the doubling effect would result in a receiving-end crest of $2 \times 3.1 = 6.2$ divisions, i.e., a 20-percent enhancement of the sending-end pulse. Note also that, while the *amplitudes* are attenuated, the *rise times* tend to be increased, so that the volt-time integral of the pulse (and therefore its potential for damaging energy-sensitive components) is not attenuated as quickly as the amplitude.

B. 2-μs Pulse

Fig. 3 shows the propagation characteristics of a 2-μs-wide pulse along the same line, with matched termination at the receiving end. For this slower pulse the attenuation is lower, with a ratio of 0.94 between the voltages of points separated by 75 m of line. The change of slope, which was quite apparent for the 200-ns pulse, is hardly noticeable in this recording, the four pulse traces having essentially parallel rises and falls. This lesser distortion is easily explained by the lesser effect of the line shunt capacitance on the lower frequencies associated with the 2-μs-wide pulse.

C. 1.2/50-μs Surge

Fig. 4 shows the test circuit for surge tests with matched terminations. The R_s series resistance at the sending end provides matching for the low-impedance (0.6 or 12 Ω) generator plug-in networks, and the R_t terminating resistance at the receiving end eliminates reflections.

Fig. 5 shows three recordings for the 75-m conduit line excited by a 1.2/50-μs surge, with open end and with a matching termination at the receiving end. Fig. 5(a) shows the

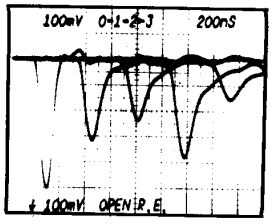

Fig. 2. Recordings at four points of line, open end, for 200-ns-wide pulse.

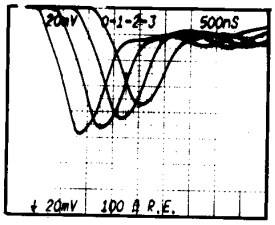

Fig. 3. Recordings at four points of line, matched termination, for 2-μs-wide pulse.

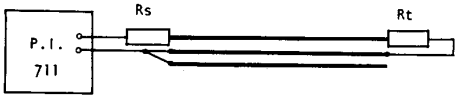

	Z_{pi}	Rs	Rt
1.2/50, Conduit	0.6	100	100
1.2/50, Non-metallic	0.6	125	125
Ring Wave, conduit	12	50	100

Fig. 4. Test circuit for recordings with 1.2/50-μs surge and with ring wave.

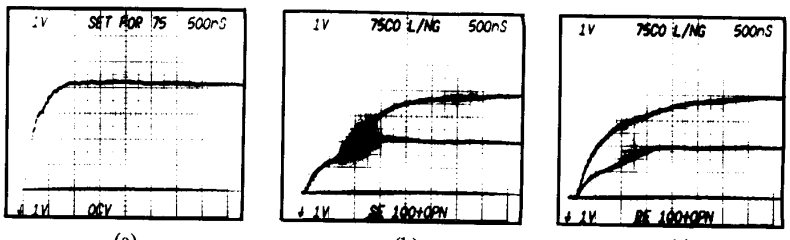

(a) (b) (c)

Fig. 5. Recordings on 75-m conduit line with 1.2/50-μs surges. All oscillograms: vertical = 1 kV/div, sweep = 500 ns/div. (a) Open-circuit voltage produced by generator. (b) Voltage at sending end. Top: open at receiving end. Bottom: 100 Ω at receiving end. (c) Voltage at receiving end. Top: open at receiving end. Bottom: 100 Ω at receiving end.

open-circuit voltage delivered by the surge generator. Because a series resistor is present at the sending end, a 2:1 voltage divider effect is produced at the sending end for the long-term voltages when a terminating resistor is connected at the receiving end. Therefore, the terminated-end trace (bottom) shows half of the voltage of the open-end trace (top). For the first 750 ns of the sweep, the reflection from the receiving end has not arrived, and, consequently, the two traces are identical. Fig. 5(c) shows the voltages at the receiving end, with and without termination. Observe that the long-term voltages match the sending-end voltages of Fig. 5(b). Only the rising part of the top trace of Fig. 5(c), for the first 1500 ns, shows a doubling of the voltage applied at the sending end, but this doubling would not change the stress at the receiving end, except for the steeper rate of rise.

The behavior of the nonmetallic (stretched) 75-m line shown in Fig. 6 is similar to that of the conduit line, but the traces are not quite as smooth. From the differences in high-frequency response of the conduit and nonmetallic line shown by the continuous-frequency measurements discussed later, these irregularities in the nonmetallic line can be expected.

D. 0.5-μs 100-kHz Ring Wave

Fig. 7 shows the recordings for the 75-m conduit line excited by a ring wave, with open end and with matched termination. The voltages at the sending end (Fig. 7(a) and (c)) differ by the reflection during the first loop, producing the double peak in Fig. 5(a). Furthermore, the voltage divider effect of the series resistance also lowers the sending-end voltage when a terminating resistor is connected at the receiving end. At the receiving end the difference between an open or terminated condition is apparent.

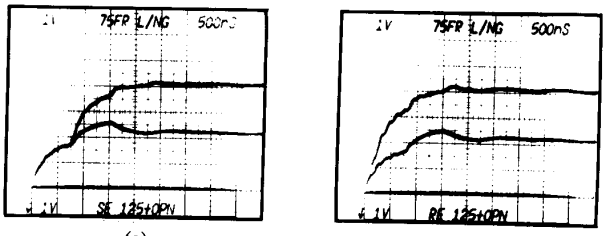

(a) (b)

Fig. 6. Recordings on 75-m nonmetallic stretched line with 1.2/50-μs surges. Vertical: 1 kV/div. Sweep: 500 ns/div. (a) Voltages at sending end. Top: open at receiving end. Bottom: 125 Ω at receiving end. (b) Voltages at receiving end. Top: open at receiving end. Bottom: 125 Ω at receiving end.

1) With a matched termination, the receiving-end voltage of the first loop is 2.5 kV for a 3-kV sending-end voltage, indicating attenuation of the high frequencies as previously noted in the case of the 200-ns pulse. Later loops show less attenuation.

2) With an open end the reflection effect is less than

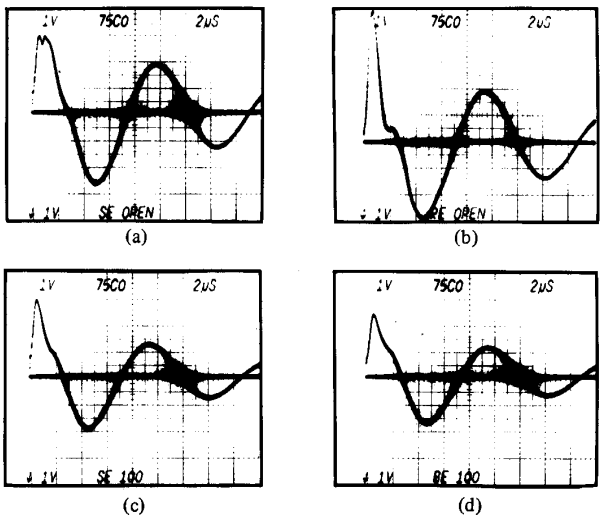

Fig. 7. Recordings on 75-m conduit line with 0.5-μs 100-kHz ring wave. All oscillograms: vertical = 1 kV/div, sweep = 2 μs/div. (a) Voltage at sending end, line open at receiving end. (b) Voltage at receiving end, line open at receiving end. (c) Voltage at sending end, 100-Ω termination at receiving end. (d) Voltage at receiving end, 100-Ω termination at receiving end.

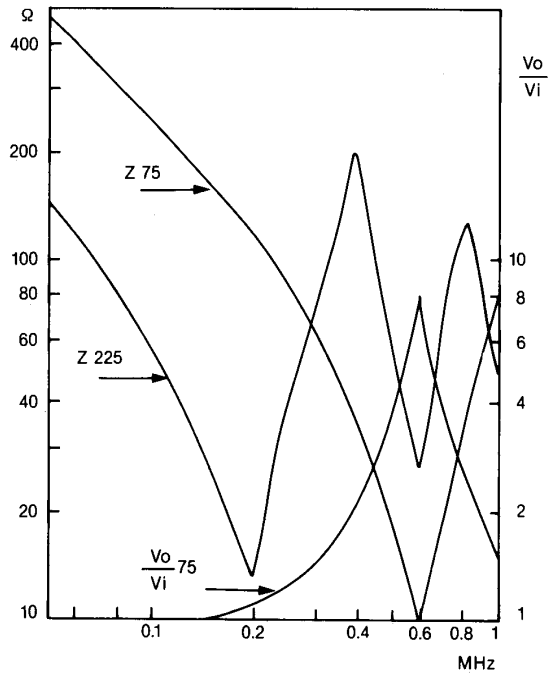

Fig. 8. Impedance of 225- and 75-m lines and V_o/V_i ratio of 75-m line as function of frequency.

doubling—5 kV against 3 kV—as the result of the high-frequency attenuation and again little attenuation in later loops.

Continuous Frequency Measurements

Two types of frequency domain measurements were performed over the frequency range of 100 Hz–10 MHz with the spectrum analyzer and tracking generator.

1) The input impedance versus frequency of the line was determined by measuring the voltage applied to the line and then the current drawn by the line.
2) The transfer ratio of the line versus frequency was determined by measuring the voltage applied to the line and the voltage at the far end of the line.

To assure adequate decoupling of the tracking signal generator output, a resistive pad was connected to the output. This pad consisted of a 47.5-Ω resistor in series with a 2.5-Ω resistor to a coaxial shield ground. The test line was thus driven by the 2.5-Ω source. All data were recorded with an X–Y recorder, and then calculations were made to establish the reported data.

The transfer ratio measurements required ungrounded instrumentation in order to eliminate ground loops and the influence of undesired grounding at the remote end of the test line. Therefore, a relatively high resistance of a 7500-Ω noninductive resistor was connected at the remote end of the test line and a Genistron current transformer was used to measure the current flowing in the resistor, thus establishing the voltage at the quasi-open-ended line. The voltage at the sending end was obtained through a Hewlett-Packard 1121A ac voltage probe.

Fig. 8 illustrates the input impedance of the conduit line under this type of excitation. The two curves labeled Z75 and Z225 show the impedance of the line seen from the sending end when a 100-Ω matching resistance is connected at the receiving end, as a function of the frequency of the applied signal.

Referring to the Z225 curve, the behavior of this 225-m line shows the standing wave effects at 1/4, 1/2, 3/4, and 1 wavelength. At 0.2 and 0.6 MHz the line impedance is low, typical of 1/4 and 3/4 wavelengths, while it is high at 0.4 and 0.8 MHz, typical of half and full wavelengths. For the 0.8-MHz frequency, the period is 1.25 μs; with a line length equal to one full wavelength, the speed of propagation determined by this measurement is 225 m/1.25 μs = 180 m/μs, which is close to the result obtained by the pulse propagation time of 1.1 μs shown in Fig. 1, i.e., 225 m/1.1 μs = 204 m/μs. The difference between these two results is well within the limits of calibration and reading of the different instruments used for the measurements.

Referring to the Z75 curve of Fig. 8, the first low point occurs at three times the frequency of the first low on the Z225 curve, which is consistent with the 1:3 ratio of line length. Note also that this shorter line involves a lower total resistance; hence the 1/4-wave resonance effect is larger than the 3/4-wave resonance. This resonance is quite apparent on the V_o/V_i 75 curve, which shows the ratio of the voltages at the receiving end to the sending end, with a quasi-open (7500 Ω) receiving end.

Fig. 9 is a plot of the input impedance versus frequency of three configurations of open-ended 75-m lines: the conduit-encased line, the nonmetallic coiled line, and the nonmetallic stretched line. The differences of input impedance for the three configurations should come as no surprise. The conduit line appears well controlled, with more damping that the

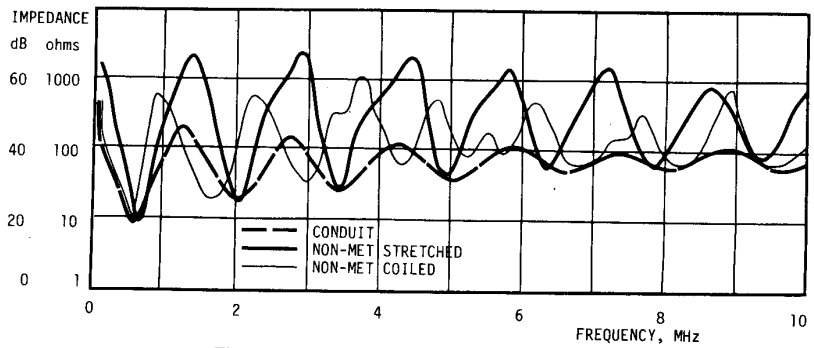

Fig. 9. Input impedance for open-ended 75-m lines.

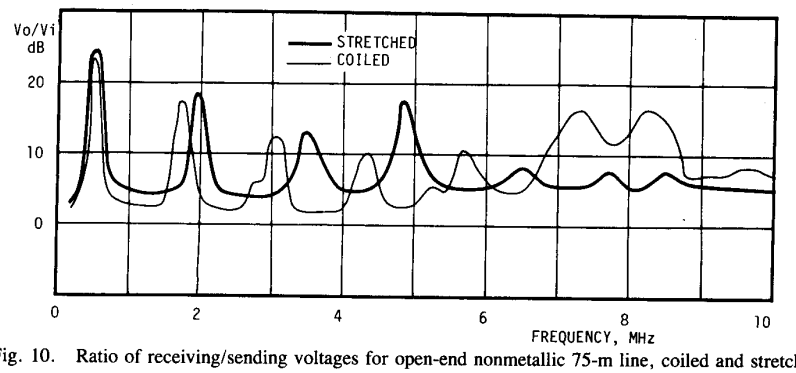

Fig. 10. Ratio of receiving/sending voltages for open-end nonmetallic 75-m line, coiled and stretched.

nonmetallic line of amplitude between the 1/4-wave minima and 1/2-wave maxima of the lines. The simple response of the conduit line is also apparent, compared to the parasitic effects that appeared in the coiled configuration.

Fig. 10 shows a comparison between coiled line and stretched line for the ratio between sending-end and receiving-end voltages. The voltage multiplication seen at the far end at about 0.6 MHz agrees with the V_o/V_i 75 curve of Fig. 8 for the 1/4-wavelength condition. Both stretched and coiled lines show a multiplication of about 24 dB (15 times) with little difference between the responses. The second peak begins to show some shift between the two lines, and the differences increase at higher frequencies, showing the need to stretch out the line for obtaining results free from the parasitic effects of the coiled configuration. The ratio drops to a minimum of 5–6 dB rather than zero (no voltage enhancement) because the measurement system used had a noise background which precluded recording of any lower current measurements at the receiving end.

Fig. 11, reproduced from [1], shows an earlier measurement of line impedance in the low-frequency region made with a Hewlett-Packard Model 4800A vector impedance meter, with the line shorted at the far (receiving) end, which is the converse situation of the measurements reported here, where the voltages at the receiving end are recorded with the line in quasi-open condition.

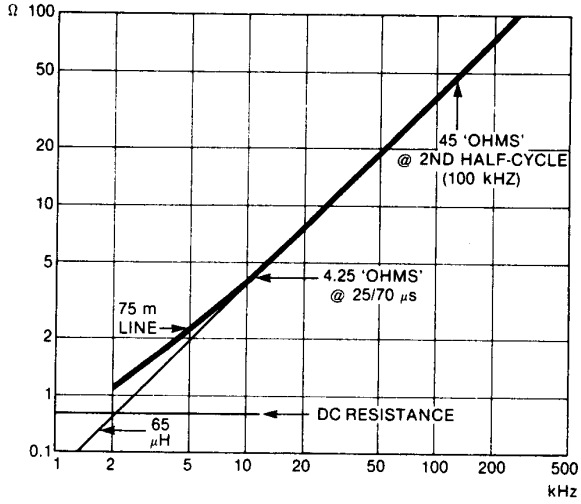

Fig. 11. Input impedance of 75-m line, nonmetallic type, with shorted receiving end.

Relations Between Impulse and Continuous Wave Measurements

The time-domain impulse measurements illustrate directly the propagation of a surge of the type encountered in actual power systems. The effects of an open end, or a high impedance at the far end, are quite apparent.

The frequency-domain measurements indicate the importance of standing wave effects for specific frequencies, which may be frequencies of low-level communication carriers or the frequency of a particular point of the transform spectrum of a single impulse. To predict performance of a particular configuration, it may then be possible to model the line, which would then become a simple case of conventional network analyses by numerical methods [2]. On the other hand, setting up a real line or network of lines may be cumbersome but

yields immediate results, such as those illustrated in the next section on the effect of connecting surge suppressors at the end of the line.

Comparisons of impulse measurements sometimes give considerable emphasis to crest values, neglecting the effect on waveform, as noted in connection with Fig. 2. A continuous-frequency spectrum, however, will readily identify the change.

Effects of Connecting a Surge Suppressor

With the advent of increasingly sophisticated electronic devices, a proliferation of add-on surge suppressors has been offered for insertion at the point of use of these devices, that is, at the receptacle located at the end of a line, such as those discussed in the preceding sections. The actual configuration of these suppressors is generally not disclosed, but they may be classified into three categories, for the case of a single-phase two- or three-wire power supply. A first category involves only one protective device, which may be connected line-to-neutral or line-to-ground. A second category would involve two devices, and the third, three devices. The differences among these three categories is shown in [1]; however, ring-wave surges [3] may present a more insidious situation than the unidirectional surges used in [1]. The insidious nature of the effect is associated with the inductive characteristics of the line discussed here, when carrying fast-rising surge *currents* associated with the presence of a surge suppressor at the end of the line.

Fig. 12 shows four possible combinations of protective devices that may be connected at the user's end of a branch circuit when the user has no control on what protection could be added at the service entrance. Fig. 12(a) shows a single protective device connected between the line and neutral conductors, under the perception that this is the location of the most sensitive components of the connected load (*L*). Fig. 12(b) shows again a single device, connected between the line and grounding conductors, under the perception that the surge current should be returned to "ground." Fig. 12(c) shows two devices, one between line and neutral conductors, the second between neutral and grounding conductors. Fig. 12(d) shows three protective devices. The effects of various connections when a slow-front current is involved were described in [1]. With faster surges, while lower energies are involved, ironically, a greater voltage spike is produced, as revealed by Fig. 13.

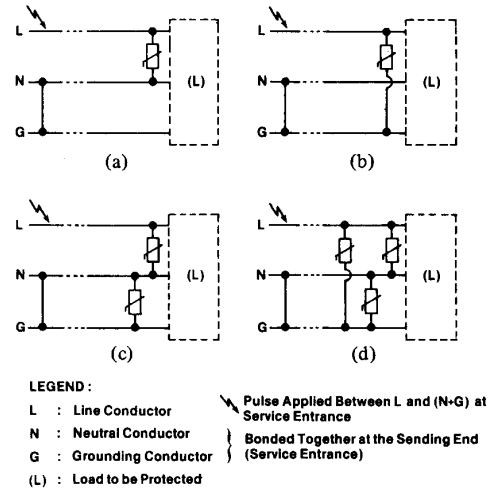

Fig. 12. Connection options for protective devices at end of branch circuit.

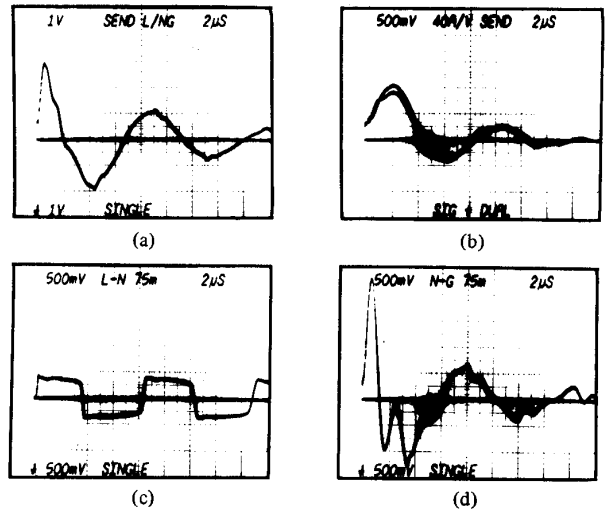

Fig. 13. Effect of connecting single surge suppressor between line and neutral at end of 75-m line, with neutral and grounding conductor bonded at origin of line. (a) Voltage at sending end while line is carrying current of Fig. 12(b). Vertical: 1 kV/div. Sweep: 2 μs/div. (b) Current in line with ring-wave surge generator excitation. Vertical: 20 A/div. Sweep: 2 μs/div. (c) Voltage between line and neutral with surge current of Fig. 12(b). Vertical: 500 V/div. Sweep: 2 μs/div. (d) Voltage between neutral and grounding conductor with surge current of Fig. 12(b). Vertical: 500 V/div. Sweep: 2 μs/div.

Fig. 13 shows the result of connecting a surge suppressor device that provided clamping only between the line and neutral conductors, as shown in Fig. 12(a). Fig. 13(a) shows the voltage set at a peak of 3 kV at the sending end of the line. With that setting of the generator, the current in the line is shown in Fig. 13(b). The generator is capable of delivering 6 kV open-circuit and 500-A short-circuit. The load-dependence of this type of circuit is evident in Fig. 13(b) where the current peak is limited to 40 A. Fig. 13(c) shows the voltage between line and neutral which, predictably, is correctly clamped at about 400 V. However, the voltage between neutral and grounding conductors (Fig. 13(d)) reaches a peak of 2300 V during the initial current rise and 1300 V during the fall of the current at the end of the first loop. The correspondence between peaks of voltage during fast current change and zero voltage during peaks of current is quite apparent in a comparison of Fig. 13(b) and (d). This correspondence is attributable to the inductive voltage drop in the neutral conductor, which elevates the neutral terminal of the line-end receptacle with respect to the grounding terminal. The grounding terminal remains at the potential of the ground at the sending end.

A load connected at the receptacle and "protected" by the single device will then be exposed to substantial peaks of voltage between its neutral and chassis, if any. Because of the expectation that neutral and grounding conductors should not

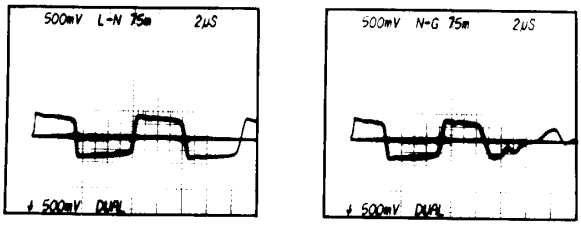

(a) (b)

Fig. 14. Effect of connecting suppressor having clamping devices between both line-neutral and neutral-ground pairs, at end of same line and same applied surge as in Fig. 13. (a) Voltage between line and neutral with surge current of Fig. 13. (b) Voltage between neutral and grounding conductor with surge current of Fig. 13.

drift far apart in voltage, being bonded at the service entrance, the designer of the load equipment might not have provided for this 2300-V peak in the insulation between neutral and chassis. If the function of the equipment can be disturbed by fast voltage changes, there is also a good probability that disturbances may occur. Thus what was intended to be a simple protective scheme can result in unwanted and unexpected problems.

An effect similar to that shown in Fig. 13 would be obtained for the connection of Fig. 12(b), but with the 400-V clamping voltage occurring between line and grounding conductors and the uncontrolled voltage of 2300 V produced between line and neutral conductors, placing any components connected across the line in severe jeopardy.

In contrast, the performance of a surge suppressor that provides clamping between line and neutral *and* between neutral and grounding conductors is shown in Fig. 14, for the same surge-injection conditions as those of Fig. 13(a) and (b). Both voltages are clamped below 400 V, and while the initial rates of voltage changes are not affected by the clamping action, the total excursion is limited. Clearly, this mode of protection with added clamping between neutral and grounding conductors offers a substantial improvement over the case of Fig. 12(a).[1] Further protection of equipment sensitive to fast voltage changes may be obtained by insertion of a filter that will decrease the rate of voltage changes shown in Fig. 14.

Implications and Conclusion

The data obtained by these measurements should be a source of useful information for the application of preventive measures for equipment connected at the end of lines, such as those reported here.

1) From the time-domain surge measurements, it becomes apparent that long lines will attenuate single-shot impulses of very short duration (less than 1 μs), but no appreciable attenuation can be expected for longer pulses.

2) An open-end line (e.g., a line feeding a low-power control circuit) will produce the classical doubling effect when the line length is sufficient to contain the surge front. If the line if shorter than this value, reflections occur while the surge front is still rising, so that the doubling effect produces steps on the front but no doubling of the ultimate peak of this surge.

3) While conduit-enclosed lines may be folded for convenience in making indoor testing, nonmetallic lines need to be stretched away from surrounding conductors to obtain valid results at high frequencies.

4) Connecting surge protective devices at the end of a line is a typical action undertaken by prudent users; however, unless the behavior of the circuit is well understood, simple protective schemes can backfire unless adequate connections are provided.

[1] This improvement is obtained from the point of view of *equipment* protection, where a surge of 1-μs duration as seen in Fig. 13(d) can cause failure. The National Electrical Code, in Section 280-22, specifically permits the connection of a surge arrester between any two conductors of a three-wire single-phase system. However, with the surge current now returning to the service entrance by the parallel combination of the neutral conductor and the grounding conductor, a brief surge will appear between the equipment chassis connected to the grounding conductor and other local grounded structures, unless a bond is installed at that point to bridge the chassis and the other local grounded structures. The occurrence of this brief surge would be limited to the duration of high rates of current change, but its implication on *personnel* safety has not yet, to our knowledge, been evaluated in this context.

References

[1] F. D. Martzloff, "The propagation and attenuation of surge voltage and surge currents in low-voltage ac power circuits," *IEEE Trans. Power App. Syst.*, vol. PAS-102, pp. 1163-1170, May 1983.

[2] H. W. Dommel, "Digital computer solution of electromagnetic transients in single and multiphase networks," *IEEE Trans. Power App. Syst.*, vol. PAS-88, pp. 388-399, Apr. 1969.

[3] *IEEE Guide for Surge Voltages in Low-Voltage AC Power Circuits*, ANSI/IEEE Standard C62.41, 1980.

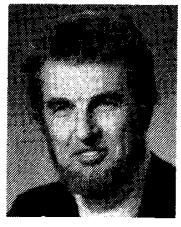

François D. Martzloff (M'56-SM'80-F'83) was born in Strasbourg, France, on June 9, 1929. He received the degree from Ecole Spéciale de Mécanique et d'Electricité, the M.S.E.E. degree from the Georgia Institute of Technology, Atlanta, and the M.S.I.A. degree from Union College, Schenectady, NY, in 1951, 1952, and 1971, respectively.

He was with the General Electric Company for many years, working on transient measurements, surge protection of electronics, and applications of varistors. He is presently with the National Bureau of Standards, Gaithersburg, MD, focusing on conducted electromagnetic interference.

Mr. Martzloff has received numerous Awards and he is active in writing standards with the IEEE, IEC, and ANSI.

Harold A. Gauper, Jr. (M'49-SM'55) received the B.S. degree in electrical engineering from the University of Wisconsin, Madison, in 1943.

He joined the General Electric Company shortly after graduation. Since his assignment to the field of Electromagnetic Compatibility in 1950, he has continued to specialize in the development of measurement methods, prediction and control of EMI, NEMP, and immunity associated with a broad range of consumer, industrial, electrical power, and military products and programs. He holds three patents on EMC-related control techniques. Among his assignments for many years was the responsibility to represent the General Electric Company interests in EMI/EMC technical standards and regulations. As a result he was, and continues to be, involved with Federal Communications Commission rulemaking with regard to Part 18 (ISM Equipment) and Part 15 (Radio Frequency Devices). He was Chairman of the NEMA Electromagnetic Compatibility Committee and active in the EMC standards work of ANSI C63, IEEE EMC Society, and other IEEE standards committees, as well as the IEC-CISPR and TC-77. He continues to be involved in IEEE EMC standards matters since his recent retirement from the General Electric Company.

Mr. Gauper has served on the IEEE EMC Society Board of Directors, most recently in 1978-1981, and served as a Charter Member of the Federal Electromagnetic Radiation Management Advisory Council which advised on RF biohazard matters.